Polarization-Insensitive Variable Optical Attenuator and Wavelength Blocker Using Liquid Crystal Polarization Gratings

Elena Nicolescu, *Student Member, IEEE,* Chongchang Mao, Amir Fardad, and Michael Escuti, *Member, IEEE*

Abstract—We demonstrate a variable optical attenuator (VOA) based on liquid crystal polarization gratings (LCPGs), which eliminates the need for complex polarization management found in competing *LC* technologies. We then configure the VOA as a multi-channel wavelength blocker resulting in a simple, compact architecture with high performance and low cost. Together with a dual fiber collimator, relay lenses, a diffraction grating, a quarter wave plate, and a mirror we achieve optical attenuation of ∼50 dB with minimal polarization dependent loss (≤0.3 dB) and insertion loss (≤2.5 dB). The device also manifests competitive wavelength flatness (≤0.35 dB variation), response times (∼40 ms), and temperature dependent loss (≥47 dB maximum attenuation up to 85°C). We describe the principle of operation, explain the fabrication process and optimization challenges, and finally present the system design and experimental results for a four-channel, 100 GHz wavelength blocker in the C-band.

Index Terms—Polarization grating, variable optical attenuator, wavelength blocker.

I. INTRODUCTION

VARIABLE optical attenuators (VOAs) have many applications in optical telecommunication networks. One example is performing the wavelength blocking function in reconfigurable optical add/drop multiplexers (ROADM). Dense wavelength division multiplexing (DWDM) networks based on ROADM have emerged as a solution to the scalability issues that plagued legacy DWDM networking techniques. ROADMs enable fast, inexpensive, automated reconfiguration of DWDM networks without the need for manual tuning or service-interrupting upgrades.

Wavelength blockers (WB), which selectively pass or block certain wavelengths, are the core components of most current ROADM systems. They consist of a multiplexer, a multi-channel VOA array, and a demultiplexer. By controlling the attenuation level of each individual channel, the WB performs dynamic channel equalization as well as individual channel blocking. Typical wavelength blockers have either 80 channels at 50 GHz spacing for long haul applications, or 32 or

40 channels at 100 GHz spacing for metropolitan applications. Here, we demonstrate a four-channel wavelength blocker with 100 GHz spacing with a system design that can easily be expanded to a 40 channel configuration.

Several competing implementations of VOAs have been proposed for use in optical networks including MEMS [1], [2], microfluidic [3], [4], planar lightwave circuit (PLC) [5], [6] and liquid crystal (LC) [7]–[9] approaches. Each of these have tradeoffs in parameters such as cost, size, response times, maximum attenuation, power consumption, polarization-dependent loss (PDL) and insertion loss (IL).

MEMs applications boast high dynamic ranges and fast response times, but suffer from high cost, complex fabrication, and alignment problems. In PLCs the disadvantages are either high power consumption and waveguide deformation at high temperatures or low attenuations due to absorption and scattering in the waveguide. A few microfluidic approaches have also been demonstrated with low power consumption, no moving parts, and simple fabrication, but they suffer from relatively poor attenuation, PDL, and response times.

LC based VOA technologies have no moving parts and are easy to fabricate, but they rely on complex polarization management, which translates to high cost, bulky packaging, and lower yield, performance and reliability. Conventional *LC* VOAs employ a uniformly aligned liquid crystal cell sandwiched between two birefringent prisms, which separate the beam into two orthogonal polarization states and then recombine it. To achieve attenuation in these systems, each polarization state must be modulated separately as it passes through the *LC* cell [10], [11].

We suggest a different *LC* approach, virtually insensitive to polarization, which uses a single diffractive *LC* element and combines the low cost and simple fabrication of *LC* devices with the high performance obtained by MEMS devices. The design is based on Liquid Crystal Polarization Gratings (LCPG) [12]–[15], which have been extensively studied for applications including microdisplays [16], tunable optical filters [17], spectrophotometers [18], and beamsteering applications [19], [20]. These are a class of thin-film diffraction gratings which operate by periodically modulating the polarization of light across the wavefront, as opposed to the conventional phase or amplitude. Note that researchers have recently studied the low-loss, polarization-insensitive switching properties of these *LC* elements in the context of displays and generic modulators [15], [21], [22]. However, here we focus on LCPGs explicitly in a fiber optics communications system device, and employ both design and characterization relevant to this context. The key properties of the LCPG for the VOA application are: (a) very high attenuation
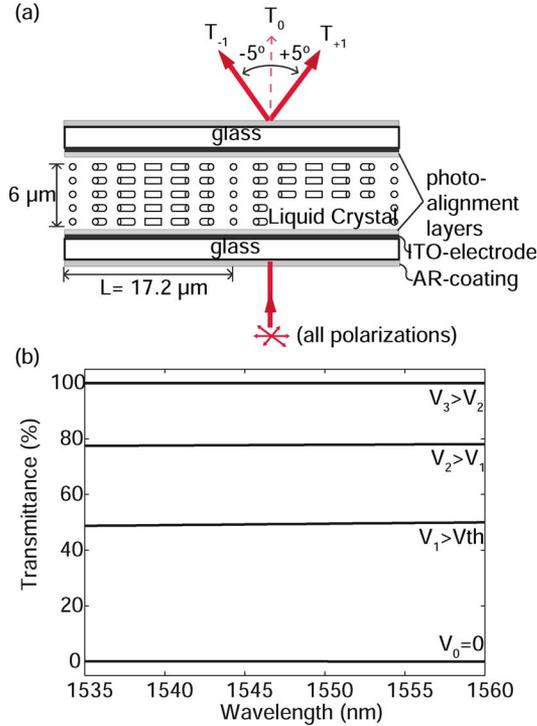
Fig. 1. (a) LCPG structure and diffraction behavior and (b) %Transmittance versus wavelength for a representative LCPG at various voltages.

and low insertion loss, (b) low polarization dependent loss, (c) fast (few milliseconds) response time and low power consumption and (d) relatively simple and inexpensive fabrication and alignment.

LCPGs are also known as anisotropic or vectorial gratings and are embodied as a spatially varying birefringence and/or dichroism. An effective way [12], [22], [23] to create this structure is using bulk nematic LCs aligned by photo-alignment surfaces that have been exposed with a polarization hologram, leading to the structure illustrated in Fig. 1(a). Note that the key parameters of an LCPG include the grating period Λ, grating thickness d, linear birefringence Δn, and voltage threshold V_{th}.

The *transmittance* (T_0) spectrum for light normally incident (within $\pm 20°$) can be expressed as [13]

$$T_0(\lambda) = K \cos^2 \left(\frac{\pi \Delta n d}{\lambda} \right) \qquad (1)$$

where T_0 is the raw transmittance of the zeroth diffracted order and λ is the vacuum wavelength of incident light. This relation is graphed in Fig. 1(b) using representative parameters for C-band operation ($\Delta n = 0.13$ and $d = 6$ μm). The notable properties of the zeroth transmitted order of the PG are: (i) it can theoretically vary from 100% to 0% depending on the retardation $\Delta n d / \lambda$; (ii) the specular transmitted intensity is independent of input polarization and Λ, (iii) with no voltage applied, the spectral minimum occurs at the desired telecomunication band wavelength ($\lambda = 1550$ nm). Light that is not coupled into the zero order is diffracted into only the ± 1 orders.

Electrical control of the diffraction efficiency occurs by decreasing the effective birefringence (in fact, $\Delta n \rightarrow \Delta n(V)$

should be substituted in (1)). As an external voltage (V) is applied, the nematic director reversibly reorients out-of-plane thereby increasing T_0 and causing some light to be coupled into the zero order. At high voltage, the grating profile is effectively erased ($T_0(\lambda) \approx 100\%$) and all of the light is coupled into the zero order. The grating profile will re-appear when the applied voltage is removed and the light will again be diffracted into the first orders. Note that for most LCs and grating periods even when d is large, the voltage threshold [24] will be designed to remain approximately 1–2 V.

In this work we report on a VOA functioning in the C-band, having at its core an LCPG that is optimized to minimize losses and maximize attenuation. We describe the principle of operation of our system, explain the design choices, fabrication process, and optimization challenges. Finally we incorporate the VOA into a four-channel, 100 GHz wavelength blocker, present the system design, and give experimental results.

II. PIRNCIPLE OF OPERATION

The VOA operation is most easily explained in transmissive mode where only two fiber collimators and one LCPG are required to implement the VOA as depicted in Fig. 2(a). All polarization management optics required in conventional *LC* VOAs are removed, thereby allowing for lower cost, more compact packaging, higher reliability and higher performance. Depending on the voltage applied to the LCPG, the input beam will be coupled into either the zero order (T_0) or the first orders. The output collimator is aligned with the zero order such that at no applied voltage the beam is diffracted away from the collimator and at high voltage it is coupled into the collimator. This mechanism is closer to the principle of operation of MEMS devices where attenuation is achieved by managing beam direction rather than polarization state. This allows us to achieve high attenuation similar to competing MEMS devices, but without the complex fabrication and alignment requirements. As opposed to conventional *LC* VOAs, this design only has one diffractive element (no polarizers or prisms) so it does not depend on complex polarization management.

However, the reflective mode yields enhanced performance in terms of dynamic range, polarization dependent loss, and wavelength flatness. We simply replace the input collimator with a dual fiber collimator and the output collimator with a mirror. Placing a quarter wave plate (QWP) between the LCPG and the mirror compensates for any residual phase retardation from the liquid crystal cell, and the reflection from the mirror, resulting in a significant reduction in PDL [8].

In order to configure the VOA into a multi-channel wavelength blocker system we design a four-channel LCPG and introduce a conventional diffraction grating in the system as seen in Fig. 2(b). The input beam from the dual fiber collimator passes through the beam expansion optics which collimate the beam and focus it onto the grating. The light is then diffracted to achieve four orders with wavelengths in the C-band at 100 Ghz spacing. The lens collimates the diffracted spectra and focuses the beams on the mirror. The beams pass through the four-channel LCPG and depending on the applied voltage on each individual channel, each of the four beams is independently attenuated to the desired level. Recall that we are dealing with the zero-order transmitted beam
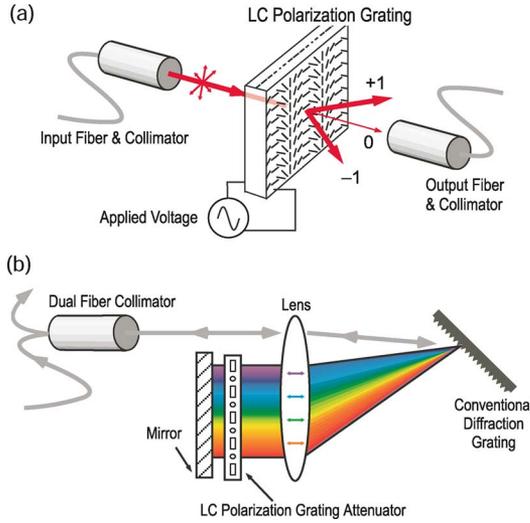
Fig. 2. Basic principle of operation for (a) a transmissive VOA system and (b) a four-channel reflective WB system.

Fig. 3. (a) Voltage response of a single LCPG at 1550 nm and (b) attenuation at various voltages as a function of wavelength.

from the LCPG which is independent of input polarization. The beam then passes through the QWP, is reflected from the mirror, and passes back through the system to be output through the dual fiber collimator.

III. LIQUID CRYSTAL POLARIZATION GRATING

A. Fabrication

The basic fabrication process of an LCPG is fairly simple [12], [22], [23]: We start with two glass substrates (1 inch × 1 inch) with a custom antireflection coating (to minimize air-glass interface reflections) and a thin index-matched ITO electrode (to minimize absorption and reflections at the electrode-LC interface). The substrates are coated with a photo-alignment material (ROP-103/2CP, from Rolic) [25], and laminated together such that a cell of uniform thickness (6 μm) is achieved. A polarization hologram is created by superimposing two coherent orthogonally circularly polarized beams from an ultraviolet laser with a small angle between them. The cell is then exposed via the polarization hologram with an energy dose of 2 J/cm^2 such that the pattern is captured in the photo-alignment layers. After exposure, the nematic *LC* fills the gap by capillary action at room temperature, and the desired LCPG structure is realized as the surfaces direct the *LC* orientation. Finally a high temperature annealing step at 150°C is used to improve the *LC* alignment and reduce defects.

The standard liquid crystal MLC-6647 from Merck was chosen for its high clearing point (∼140°C). This *LC* has birefringence $\Delta n \sim 0.13$ which requires that the cell gap be 6 μm in order to align the spectral minimum at 1550 nm based on (1). We also chose a grating period of $\Lambda = 17.2$ μm based on Elastic-Continuum theory [24] and LCPG optical models [13] which suggest that the the maximum first-order diffraction angle likely to support a defect-free LCPG structure is around ±7 degrees. We chose ±5 degrees as the convenient angle which would allow us to assemble the optical breadboard using standard optics and hardware.
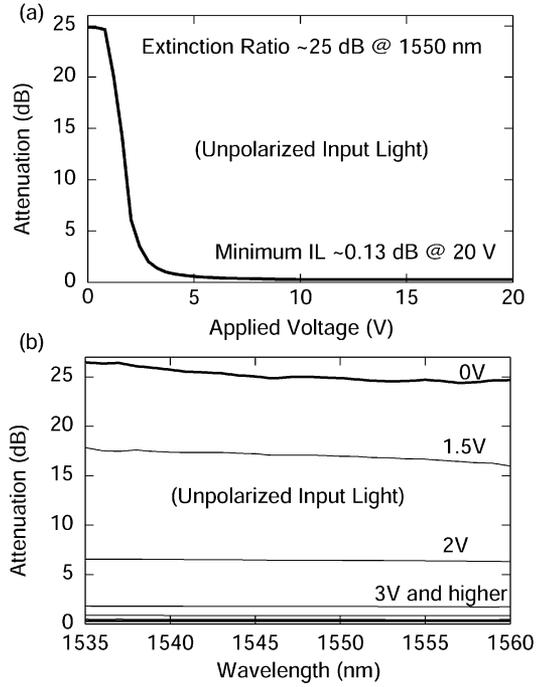
B. Results

The behavior of typical LCPGs fabricated with the methods described above is summarized in Figs. 3 and 4. The voltage response for unpolarized input light at 1550 nm is given in Fig. 3(a) showing attenuation of approximately 25 dB with a minimum insertion loss of only 0.13 dB. Fig. 3(b) shows the attenuation of an LCPG measured with a Perkin-Elmer specrophotometer between 1535 nm and 1560 nm. Each curve represents the attenuation at a particular voltage. Note that this is an analog modulator and any attenuation value between the minimum and maximum can be achieved by adjusting voltage. Also, Fig. 3(a) represents the values at 1550 nm in this plot. Note the attenuation varies slightly at any one voltage in general due to the chromatic dispersion in (1). The attenuation versus voltage for all wavelengths is substantially the same, as we will show in Fig. 6.

The polarization dependent loss (PDL) is given as a function of maximum attenuation in Fig. 4(a). For attenuations less than 15 dB, PDL remains below 1 dB. Wavelength flatness is calculated as the maximum minus the minimum attenuation values in the wavelength range 1535–1560 nm and is graphed as a function of voltage in Fig. 4(b). Our initial tests showed *LC* switching times of ∼40 ms (1 ms rise time and 39 ms fall time), which can be significantly decreased by changing the *LC* material as outlined in the Discussion section.

IV. MULTICHANNEL WAVELENGTH BLOCKER DESIGN AND RESULTS

A. Design

In order to implement the multi-channel wavelength blocker, we designed an optical system using the Zemax optical simu-
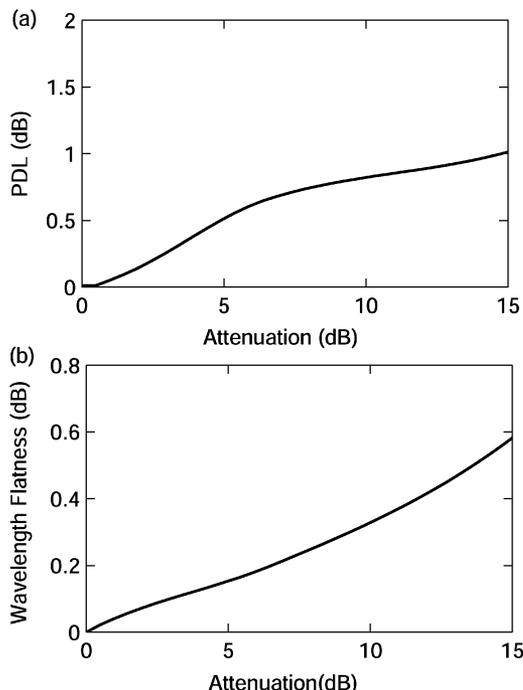
Fig. 4. (a) PDL versus Attenuation for a single LCPG and (b) wavelength flatness versus attenuation.
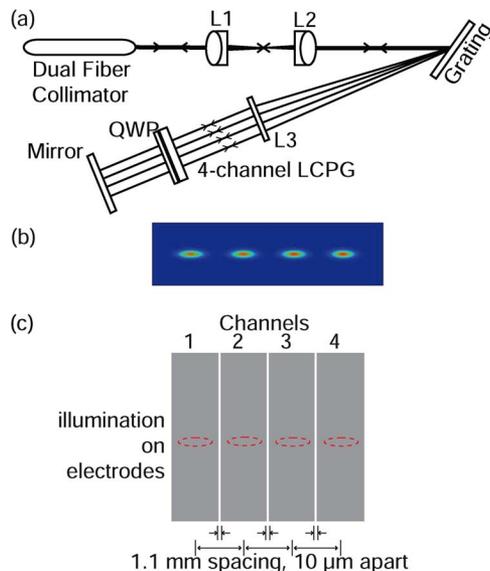

Fig. 5. (a) Detailed system design of the 4-channel system, (b) IR image of the separation of orders due to the 1200 lines/mm grating, and (c) design and layout of the four-channel LCPG.

lation tool as shown in Fig. 5(a). We selected OZ-Optics dual fiber collimators with an approximate Gaussian mode output with ∼0.4 mm beam diameter and ∼4.7 mrad (∼0.27°) full divergent angle. The dual fiber collimator working distance is greater than 10 cm. The first collimating lens has focal length of 10 cm and the other two lenses have focal lengths of 20 cm. All of the lenses in the system are AR coated and optimized for the C-band.

We chose four wavelengths in the C-band with 100 GHz spacing: 1548 nm, 1548.8 nm, 1549.6 nm, and 1550.4 nm. Optical simulations suggested that gratings of at least 900 lines/mm should be suitable for resolving the four wavelengths for the designed system. We chose a grating with 1200 lines/mm (Edmund Optics) for our design. Fig. 5(b) shows the separation of the orders at the LCPG location due to the 1200 lines/mm grating. The images were captured by an IR camera located at the plane of the LCPG. The center-to-center spacing between the orders according to simulation should be 1.08 mm, 1.1 mm, and 1.135 mm.

An LCPG with four independently-controlled channels is achieved by etching the electrode on one of the substrates into the appropriate pattern. The second ITO substrate is not patterned and serves as a common ground electrode for all four channels. All other materials and fabrication steps are the same as before. Fig. 5(c) shows the four channels, their size and spacing, and the expected locations of the beams passing through them. The electrode patterning is done with conventional photo-lithography processes using a chrome shadow mask (Photo-Sciences Inc.) The ITO is etched using a standard reactive-ion-etching (RIE) technique.

The channels of the LCPG are independently controlled by a voltage modulated at 4 kHz applied by a B1020 Meadowlark

voltage controller. Sample temperature is controlled by a HP 6205C dual DC power supply and monitored on an Omega display. PDL was measured using a PS3 PDL Multimeter. Wavelength flatness is measured using an AQ6317B spectrum analyzer and a broadband ASE light source (1530–1610 nm).

The system was assembled on a 16 inch by 18 inch breadboard for testing and measurement purposes. However, the optical system was designed such that the size can be reduced to a compact ∼17 cm × 6 cm module.

B. Results

The reflective system with the QWP compensation exhibits a significant improvement in maximum attenuation and PDL over the single PG results. Fig. 6(a) shows the voltage response of all four channels of the wavelength blocker on the same plot. We notice that the characteristics of the channels are nearly identical to each other. The turn-on voltages are approximately 1.5 V, the maximum attenuation for all four channels is 50 dB, and the insertion loss for the entire system is 2.5 dB. Fig. 6(b) shows the attenuation characteristics of the four channels as a function of channel wavelength. Each curve represents the attenuation at a particular voltage.

Fig. 7(a) shows the PDL characteristic as a function of attenuation for all four channels. The PDL remains under 0.3 dB for attenuations up to 30 dB. There are slight variations in PDL for individual channels, and we can see a general trend of slight PDL increase with increasing attenuation.

To measure the cross-talk between channels, a high voltage (20 Vrms) is applied to each channel in turn while the input wavelength is maintained constant. The change in collected power through the dual fiber collimator is monitored as each channel is turned on then off, and the adjacent channel is then turned on and off (without changing wavelength). The power cross-talk between channels was below our measurement noise floor (< -75 dB).
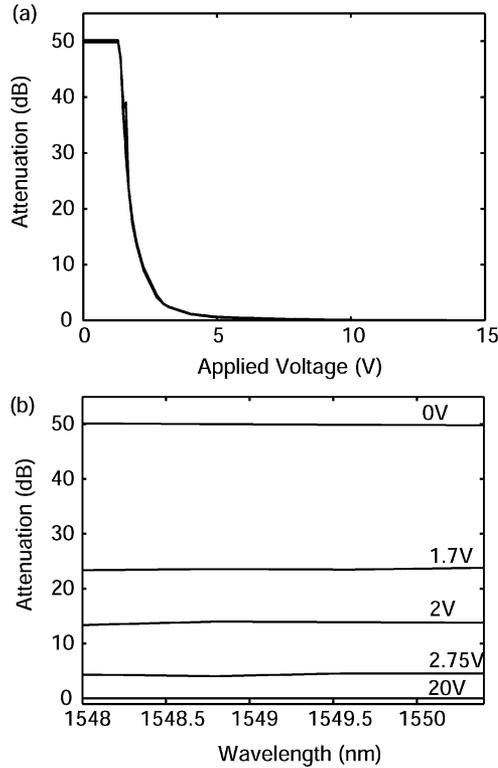
Fig. 6. (a) Voltage response of all four channels shown on the same axes and (b) attenuation versus wavelength characteristic at various voltages. All four channels are shown in (a), but their responses are nearly identical, as supported by the spectra in (b).

For optical communications applications it is important to also consider how the device functions under varying temperature conditions. We tested our samples from 22°C to 85°C at room humidity. Since all channels have very similar behavior, in Fig. 7(b) we show the results for the temperature experiment on channel 1. It is evident that within a reasonable temperature range the optical properties of the device are not significantly effected. Even at the highest temperature the maximum attenuation was above 47 dB. We also performed single pass, transmissive mode tests in the temperature range of −40°C to 85°C. The insert to Fig. 7(b) shows the change in the maximum attenuation state with temperature. Here again we see that the maximum attenuation varies by less than 2.5 dB over the normal operational range of the device (−5°C −75°C).

Finally, we explored the wavelength flatness (or wavelength dependent loss) of the system. Fig. 7(c) depicts the wavelength flatness of channel 3 as a function of attenuation. Note that the dotted line is a least squares regression meant to guide the eye. We see that for attenuations between 0.5 dB and 15 dB the spectrum is flat to within 0.35 dB.

V. DISCUSSION

Slight variations in the fabrication process of the LCPG can significantly impact the key optical properties of the device including insertion loss (IL), maximum attenuation and polarization dependent loss (PDL). We experimentally optimized the fabrication in order to improve these properties. To minimize
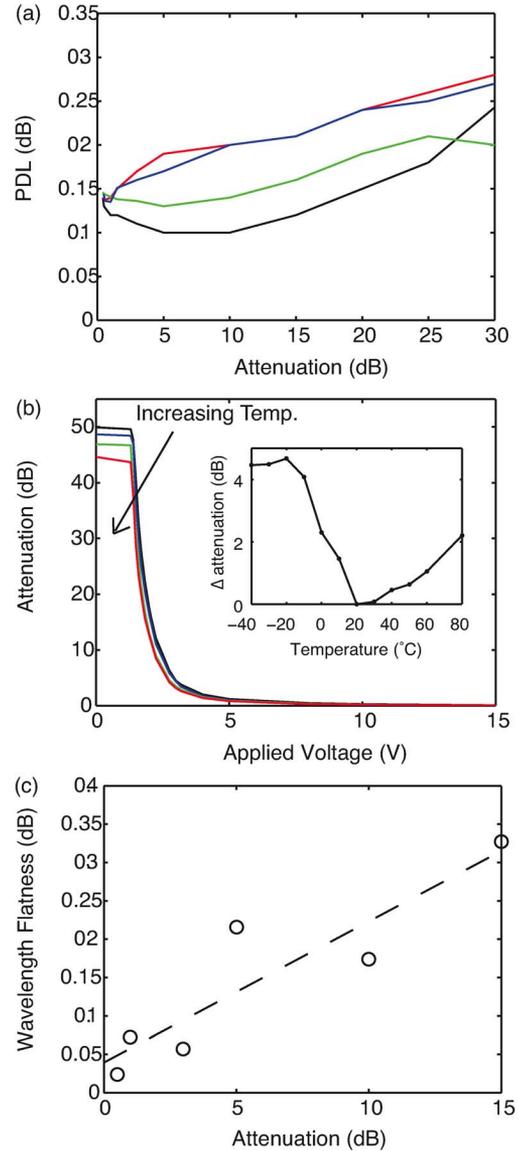

Fig. 7. (a) PDL versus attenuation for all four channels. (b) TDL vs applied voltage at 22°C, 48°C, 66°C, and 85°C. Insert shows change in the maximum attenuation state with temperature varying between −40°C to 80°C for a single pass transmissive system. (c) Wavelength flatness as a function of attenuation where the dotted line is a least squares regression.

IL we used glass substrates with a custom antireflection coating (to minimize air-glass interface reflections) and a thin index-matched ITO electrode (to minimize ITO absorption and reflections at the electrode-LC interface). To optimize maximum attenuation and PDL we studied the exposure dose (fluence = power × time), cell gap uniformity, *LC* fill temp, *LC* anneal process, and intensity and polarization-states of the recording beams. Best results were achieved when (a) the recording beams are of equal intensity and the polarization state of each beam is as circular as possible, (b) the exposure dose is greater than 2 J/cm^2, (c) the *LC* is filled at room temperature, and (d) a high temperature annealing step at 150°C is added after filling. These steps are meant to increase the anchoring strength of the photo-alignment layer as well as reduce the amount of defects within the *LC* layer.

The response time of the LCPG is directly related to two properties of the LC: viscosity and birefringence. By choosing a less viscous *LC* with higher birefringence we can achieve the same retardation with a smaller cell gap and therefore much faster response times. The other constraint on the choice of *LC* is its thermal behavior (particularly its clearing point). We chose the MLC-6647 since it had a high clearing temperature, but from previous work with *LC* devices at the 1550 nm wavelength we know that infrared-optimized LCs can be obtained from Merck and other vendors. For example, nematic LCs BL038 or E44 (Merck) have birefringence values close to 0.3 at 1550 nm, which enable a smaller cell gap than we employed here, and likely enable 10 ms switching times.

Throughout the execution of the project over several months, multiple devices were fabricated and tested both in the single pass transmissive mode as well as the double pass reflective mode. We did not observe any degradation of the switchable element during our experiments that would cause concern about the reliability or repeatability of the device. Having demonstrated the concept and characterized its initial performance, it is clear that full reliability testing is warranted and modest performance improvements are necessary before commercialization.

VI. Alternate Design Possibilities

We explored three other design possibilities whose results are important to this discussion even though they were not implemented in our final design. First, we fabricated and tested LCPGs with smaller diffraction angle (3 degrees instead of 5 degrees). We know that increasing the grating pitch (reducing diffraction angle) usually results in better alignment and higher anchoring strength and our experimental results did indeed show a decrease in PDL and a increase in attenuation for samples with 3 degree diffraction angle. We did not implement these components in the final system since the improvement in quality was not substantial enough to merit a redesign of the measurement system with potentially more expensive custom optics that can handle the small diffraction angle.

In an effort to further improve PDL, we also explored LCPGs that have a chiral-twist in the thickness dimention of the film. We studied primarily the Broadband PG structure as described in [26] but found that the PDL was not as good as our current non-twist LCPG approach.

Finally we explored a polymer PG construct composed of a tunable halfwave plate *LC* cell sandwitched between two polymer PGs. Polymer PGs have the same properties as conventional LCPGs except they are not switchable by applied voltage which means they have the potential to have less defects and better alignment. The modulation is achieved by electrically changing the birefringence of the halfwave plate. Additional retardation compensation films can also be added to the stack to improve optical properties. However we found that this design did not show any improvement in PDL or maximum attenuation and the conventional LCPG is still the most favorable for our application.

VII. Conclusion

In conclusion, we have successfully designed and demonstrated a polarization-insensitive VOA based on LCPGs, which were optimized for performance in the C-band. The VOA showed attenuation of ∼25 dB, minimum insertion loss of 0.13 dB, PDL below 1 dB, and switching times of ∼40 ms. We incorporated the VOA into a four-channel 100 GHz wavelength blocker in the C-band with optical attenuation of ∼50 dB, PDL below ≤0.3 dB and insertion loss of approximately ≤2.5 dB. The system also exhibits wavelength flatness to within 0.35 dB, response times of approximately 40 ms (which can be significantly improved by using an *LC* that is optimized for the IR), and minimal temperature dependent loss (≤3 dB decrease in maximum attenuation).

References

[1] C. Lee, F. Hsiao, T. Kobayashi, and K. Koh, "A 1-v operated mems variable optical attenuator using piezoelectric pzt thin-film actuators," *IEEE J. Sel. Topics Quantum Electron.*, vol. 15, no. 5, pp. 1529–1536, Sep./Oct. 2009.

[2] K. Isamoto, K. Kato, A. Morosawa, C. Chong, H. Fujita, and H. Toshiyoshi, "A 5-v operated mems variable optical attenuator by soi bulk micromachining," *IEEE J. Sel. Topics Quantum Electron.*, vol. 10, no. 3, pp. 570–578, May/Jun. 2004.

[3] L. Zhu, Y. Huang, and A. Yariv, "Integrated microfluidic variable optical attenuator," *Opt. Exp.*, vol. 13, no. 24, pp. 9916–9921, 2005.

[4] M. Lapsley, S. Lin, X. Mao, and T. Huang, "An in-plane, variable optical attenuator using a fluid-based tunable reflective interface," *Appl. Phys. Lett.*, vol. 95, 2009, 083507.

[5] Y. Xu, M. Uddin, and P. Chung, "Fabrication of a polymer based variable optical attenuator using liquid crystal cladding on inverted channel waveguide structure," in *Proc. Opto-Electron. Commun. Conf.*, Jul. 2008, pp. 1–2.

[6] K. Leosson, T. Rosenzveig, P. Hermannsson, and A. Boltasseva, "Compact plasmonic variable optical attenuator," *Opt. Exp.*, vol. 16, no. 20, pp. 15 546–15 552, 2008.

[7] Y. Wu, X. Liang, Y. Lu, F. Du, Y. Lin, and S. Wu, "Variable optical attenuator with a polymer-stabilized dual-frequency liquid crystal," *Appl. Opt.*, vol. 44, no. 20, pp. 4394–4397, 2005.

[8] X. Wang, Z. Huang, J. Feng, X. Liang, and Y. Lu, "16.3: High contrast liquid crystal modulator based on phase compensation technique," in *Proc. Int. Display Res. Conf.*, Sep. 2008, pp. 1–4.

[9] X. Liang, Y. Lu, Y. Wu, F. Du, H. Wang, and S. Wu, "Dual-frequency addressed variable optical attenuator with submillisecond response time," *Jpn. J. Appl. Phys.*, vol. 44, no. 3, pp. 1292–1295, 2005.

[10] C. Mao, M. Xu, W. Feng, T. Huang, K. Wu, and J. Liu, "Liquid crystal applications in telecommunication," *Proc. SPIE*, vol. 5003, pp. 121–129, 2003.

[11] C. Mao, M. Xu, W. Feng, J. Liu, and J.-C. Chiao, "Liquid crystal optical switches and signal processors," *Proc. SPIE*, vol. 4852, pp. 63–70, 2001.

[12] L. Nikolova and T. Todorov, "Diffraction efficiency and selectivity of polarization holographic recording," *J. Mod. Opt.*, vol. 31, pp. 579–588, 1984.

[13] C. Oh and M. Escuti, "Numerical analysis of polarization gratings using the finite-difference time-domain method," *Phys. Rev. A*, vol. 76, pp. 1–8, Jan. 2007.

[14] C. Provenzano, P. Pagliusi, and G. Cipparrone, "Highly efficient liquid crystal based diffraction grating induced by polarization holograms at the aligning surfaces," *Appl. Phys. Lett.*, vol. 89, 2006, 121105.

[15] S. R. Nersisyan, N. V. Tabiryan, D. M. Steeves, and B. R. Kimball, "Optical axis gratings in liquid crystals and their use for polarization insensitive optical switching," *J. Nonlinear Opt. Phys. Mater.*, vol. 18, no. 1, pp. 1–47, 2009.

[16] R. Komanduri, C. Oh, and M. Escuti, "34.4: Late-news paper: Polarization independent projection systems using thin film polymer polarization gratings and standard liquid crystal microdisplays," in *Proc. SID Symp.*, Apr. 2009, vol. 40, pp. 487–490.

[17] E. Nicolescu and M. Escuti, "Polarization-independent tunable optical filters based on bilayer polarization gratings," *Proc. SPIE*, vol. 7050, 2008, 705018.

[18] E. Nicolescu and M. Escuti, "Compact spectrophotometer using polarization-independent liquid crystal tunable optical filters," *Proc. SPIE*, vol. 6661, 2007, 666105.

[19] J. Kim, C. Oh, M. Escuti, L. Hosting, and S. Serati, "Wide-angle, non-mechanical beam steering using thin liquid crystal polarization gratings," *Proc. SPIE*, vol. 7093, 2008, 709302.

[20] C. Oh, J. Kim, J. Muth, S. Serati, and M. Escuti, "High-throughput, continuous beam steering using rotating polarization," *IEEE Photon. Technol. Lett.*, vol. 22, no. 4, pp. 200–202, Feb. 2010.

[21] W. M. Jones, B. L. Conover, and M. J. Escuti, "Evaluation of projection schemes for the liquid crystal polarization grating operating on unpolarized light," in *SID Symp. Dig.*, 2006, vol. 37, pp. 1015–1018.

[22] M. Escuti and W. Jones, "A polarization-independent liquid crystal spatial light modulator," *Proc. SPIE*, vol. 6332, no. 63320M, 2006.

[23] J. Eakin, Y. Xie, R. Pelcovits, M. Radcliffe, and G. Crawford, "Zero voltage freedericksz transition in periodically aligned liquid crystals," *Appl. Phys. Lett.*, vol. 85, pp. 671–673, 2004.

[24] R. Komanduri and M. Escuti, "Elastic continuum analysis of the liquid crystal polarization grating," *Phys. Rev. E*, vol. 76, no. 2, 2007, 021701.

[25] M. Schadt, H. Seiberle, and A. Schuster, "Optical patterning of multi-domain liquid-crystal displays with wide viewing angles," *Nature*, vol. 381, pp. 212–215, May 1996.

[26] C. Oh and M. Escuti, "Achromatic diffraction from polarization gratings with high efficiency," *Opt. Lett.*, vol. 33, no. 20, pp. 2287–2289, 2008.

Elena Nicolescu received the B.S. degree in electrical and computer engineering from North Carolina State University (NCSU), Raleigh, NC, in 2006, where she is currently pursuing the Ph.D. degree in the Electrical and Computer Engineering Department.

As part of the Opto-electronics and Lightwave Engineering group (OLEG) at NCSU, her research involves theoretical analysis and experimental work with liquid crystal polarization gratings for tunable optical filters and telecommunications applications.

Michael J. Escuti received the Ph.D. degree in electrical engineering from Brown University, Providence, RI, in 2002.

Since 2004, he has been an Assistant Professor of electrical and computer engineering at North Carolina State University, Raleigh, NC, where he pursues multidisciplinary research topics in photonics, flat-panel displays, diffractive optics, polarimetry, remote sensing, and organic electronics. Prior to this, he spent two years with the functional-polymers group at Eindhoven University of Technology, The Netherlands, as a Postdoctoral Fellow. He has nine received or pending patents. He has published more than 68 refereed journal and conference publications and has presented 12 invited research talks.

Prof. Escuti received the Faculty Early Career Development (CAREER) Award from the National Science Foundation in 2010. He also received the Glenn H. Brown Award (2004) from the International Liquid Crystal Society and the OSA/New Focus Student Award (2002) from the Optical Society of America at the CLEO/QELS Conference for his Ph.D. research on electrooptical materials and their use in photonics and flat-panel displays.